

Auger recombination of excitons in semimagnetic quantum dot structure in a magnetic field

A. V. Chernenko,* P. S. Dorozhkin, V. D. Kulakovskii, and A. S. Brichkin
Institute of Solid State Physics, RAS, 142432, Chernogolovka, Russia

S. V. Ivanov and A. A. Toropov
Ioffe Physico-Technical Institute, RAS, 194021 St. Petersburg, Russia

(Received 13 October 2004; published 1 July 2005)

Magnetoluminescence of CdMnSe-ZnSe disk-shaped quantum dots in a magnetic field up to 11 T is measured in the Faraday and Voigt geometries at liquid He temperatures and various levels of laser excitation. Within the range of $B=0-11$ T the intensity of the quantum dot photoluminescence increases strongly (up to two orders of magnitude) in the Faraday geometry and only slightly (~ 1.5 times) in the Voigt geometry. To explain the observed dependence on magnetic field direction the selection rules for the Auger recombination of excitons with excitation of Mn-ion are revised. The magnetic field dependence of the quantum yield of quantum dot exciton emission and its anisotropy are shown to appear due to the dependence of Auger recombination of uncharged excitons with excitation of Mn-ion on the spin of both exciton and Mn-ion. The anisotropy is provided by a quick spin relaxation of photoexcited excitons into the ground state which spin structure depends on the direction of the magnetic field.

DOI: [10.1103/PhysRevB.72.045302](https://doi.org/10.1103/PhysRevB.72.045302)

PACS number(s): 75.75.+a, 75.50.Pp, 78.67.Hc

I. INTRODUCTION

Incorporation of Mn atoms into II-VI semiconductors modifies their magneto-optical properties. Besides effects related with the carriers-Mn-ions exchange interaction such as a giant Faraday rotation and a strong Zeeman shift, it was found that even a small content of Mn introduced in a II-VI semiconductor material can strongly suppress photoluminescence (PL) if the energy gap E_g exceeds the energy of the Mn internal transition.

Recent progress in the molecular-beam epitaxy (MBE) growth of self-assembled quantum dots (QDs) makes it possible to fabricate semimagnetic semiconductor [also known as diluted magnetic semiconductor (DMS)] QDs and stimulates their intensive studies.¹ Magneto PL studies of DMS QDs^{2,3} with $E_g > 2.1$ eV have shown that similar to QW structures the quantum efficiency of QDs depends strongly on magnetic field: PL signal increases strongly (more than one order of magnitude) in the high magnetic field perpendicular to the disk-shaped QD plane. The effect has been explained by the model of the spin-dependent Auger recombination of exciton with the simultaneous excitation of Mn-ion from the ground state to the lowest excited one suggested by Abramishvili *et al.*⁴ and developed by Nawrocki *et al.*⁵ In the framework of this model, the transition of an electron from the conduction to the valence band occurs without change of its spin, and the transition is allowed if the total spin of the combined system of Mn ion+electron conserves. In particular, no Auger recombination is possible with participation of Mn-ions ground state with spin $S=5/2$ and its projection $S_z=\pm 5/2$ since the excited state has the spin $S=3/2$ and $|S_z|\leq 3/2$. The suppression of the Auger recombination in the high magnetic field is explained by the thermalization of Mn ions in the lowest state with $S_z=5/2$. The model does not take into account the hole orbital moment and, hence, predicts no dependence of the Auger recombination probability on the magnetic field direction.

However, recent studies^{6,7} revealed a strong dependence of the exciton quantum efficiency in DMS QDs and quantum wells (QWs) on the direction of magnetic field. In particular, it was found that the magnetic field parallel to the QW(QD) plane influences the energy transfer from exciton to Mn-ion much weaker than that normal to the QW(QD) plane. Falk *et al.*⁶ refused the model from Nawrocki *et al.*⁵ and explained anisotropy observed in QWs in the framework of recombination of excitons bound to neutral donors or negatively charged trions. The strong increase in the quantum yield of the QW emission with magnetic field is explained by the dissociation of D^0X centers in magnetic field when the energy of electron in spin-excited state in D^0X centers approaches its binding energy. The magneto-optical anisotropy in the model appears due to dependence of D^0X radiative lifetime on the magnetic field direction expected from the quantization of the hole spin normal to the QW plane.

In this paper we discuss the QD exciton recombination with energy transfer to Mn ions in CdMnSe-ZnSe self-assembled disc-shaped QDs in magnetic fields perpendicular to the QD plane $\mathbf{B}\parallel\mathbf{0z}$ ("Faraday" geometry) and parallel to it $\mathbf{B}\perp\mathbf{0z}$ ("Voigt" geometry). We observe the strong increase of the QD exciton emission intensity in the Faraday and a very weak one in the Voigt geometries. As mentioned above the magnetic field anisotropy is in contradiction with a simplified model of Nawrocki *et al.*⁵ The anisotropy cannot be explained as well within the model including D^0X as was suggested for CdMnSe-ZnSe QWs by Falk *et al.*⁶ To describe the anisotropy in the magnetic field dependence of the QDs exciton emission we analyzed the selection rules for the direct energy transfer from excitons with total moment $J=1$ ("bright") and 2 ("dark") to Mn ions and found that these are completely different. The Auger recombination of the bright exciton is allowed only with the conservation of Mn ion spin projection S_z that is in accordance with the suggestion of Nawrocki *et al.*⁵ In contrast, the Auger recombination of the dark exciton occurs with changing of the Mn

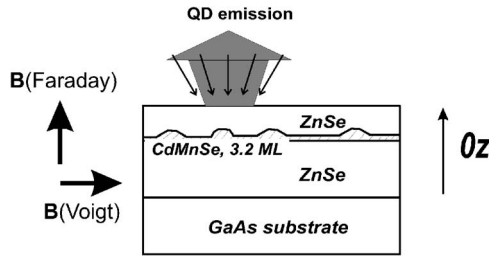


FIG. 1. A sketch of the sample under study. Directions of the magnetic field in “Faraday” and “Voigt” geometries are shown by arrows.

ion spin projection $\Delta S_z = \pm 1$. The suppression of the Auger recombination in the Faraday geometry is connected with the fast relaxation of photoexcited excitons into the lowest bright exciton state. In the Voigt geometry magnetic field mixes bright and dark exciton states. It is the admixture of $J=2$ spin state that leaves the Auger recombination allowed in this case. The decrease of the fraction of $J=2$ states in the lowest exciton state with B leads to the corresponding increase of the exciton emission.

The paper is organized as follows: In the next section we describe the samples and the experimental setup. The experimental results are described in the Sec. III. In Sec. IV we develop the theory of the Auger process for excitons. Section V is devoted to the comparison of the experimental results with the theory.

II. EXPERIMENT

The CdMnSe-ZnSe sample shown in Fig. 1 was grown by MBE pseudomorphically on a GaAs(001) substrate. A nominal thickness of the CdMnSe QD layer was 3.2 monolayers. The Mn content was $x=0.07$. The sample was immersed in superfluid He (bath temperature $T_{\text{bath}} \approx 1.8$ K) in a cryostat with superconducting magnet. PL was excited with ultraviolet lines of Ar⁺-ion laser ($\lambda=351\text{--}364$ nm). A pulse laser ($\lambda=387$ nm) with pulse-width ~ 1 ps and repetition rate 76 MHz was used for the detection of Mn PL. The laser light was focused into the spot $\sim 50 \times 50$ μm . The PL signal was dispersed by a monochromator with a 600 gr/mm grating and detected by a nitrogen cooled CCD camera.

III. MAGNETOLUMINESCENCE OF QD EXCITONS IN FARADAY AND VOIGT GEOMETRIES

PL spectra of CdMnSe QDs in the Faraday and Voigt geometries are displayed in Figs. 2(a) and 2(b), respectively. The emission originates from the radiative recombination of excitons localized in multiple CdMnSe QDs.^{8,9} The maximum of the PL line in the Faraday geometry exhibits a strong red Zeeman shift shown in Fig. 3 and a large increase of the intensity I . This behavior is typical for exciton emission in DMS QWs and QDs.^{2,3,6} The ratio $I(B)/I(0)$ increases with lowering of the excitation power P . At $P=0.1$ mW it reaches 120 times. In contrast, the increase of PL intensity with magnetic field in the Voigt geometry is weak even at low excitation energy. That is shown in Figs. 2(b) and 4.

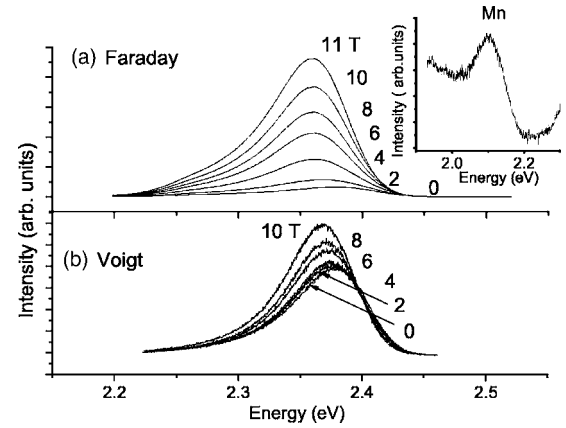


FIG. 2. PL spectra of the CdMnSe-ZnSe QDs sample at the laser excitation power 4 mW in the (a) Faraday and (b) Voigt geometries. PL signal of Mn ions internal transitions recorded under $P \approx 0.8$ mW ps laser excitation is shown in the insert.

The internal transitions from T_1 to A_1 state of Mn ions in CdMnSe have the energy in the range of 2–2.15 eV.^{2,3,6,10} PL spectra from our sample under cw excitation show a broad and very weak band in this range located on a rather strong background originated from barrier layers. To increase the relative contribution from Mn-ion emission we used pump excitation. The spectrum recorded under an excitation with ps pulsed laser is shown in Fig. 2. It displays an emission band with a half width of ~ 200 meV. The increase in the relative intensity of Mn ions under the pulse excitation compared to cw is connected with the fact the Mn luminescence is characterized by a much longer decay time than the other channels contributing to the same spectral range. The behavior of Mn PL is qualitatively similar to that observed in Ref. 6, namely, its intensity in the Faraday geometry decreases markedly already in magnetic fields of 2–4 T. No quantitative analysis is possible due to a small magnitude of this band in magnetic field and the strong increase of the background with B .

To obtain an additional information on the QD exciton emission we investigated exciton emission polarization. Fig-

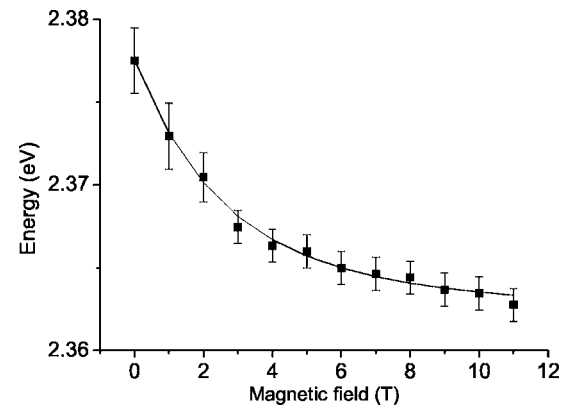


FIG. 3. The Zeeman shift of the PL signal vs magnetic field in the Faraday geometry at the laser excitation power $P=4$ mW. The solid line is the fit by Eq. (11) with parameters $B_{\text{ex}}=2.6$ T, $T_{\text{eff}} \approx 7$ K, $E_{\text{mp}} \approx 17$ meV, $E_0 \approx 2.39$ eV.

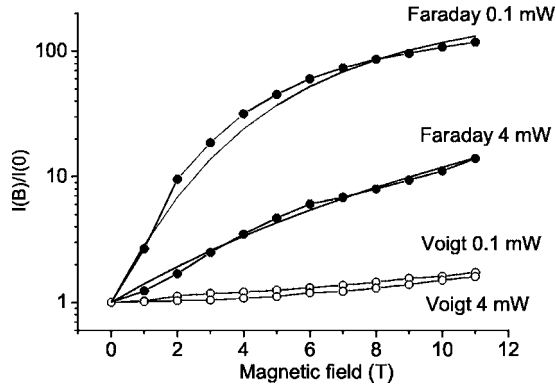


FIG. 4. PL intensity $I(B)/I(0)$ vs magnetic field in Faraday and Voigt geometries at various laser excitation powers. The solid lines show the results of the fitting with the use of Eq. (7). The best fit was found at $T \approx 2.4$ K for the $P=0.1$ mW and at $T \approx 6.5$ K for the $P=4$ mW curves. Parameters $N_A \tau_0 W_{1,-3/2} = 7.2 \times 10^7$ and $N_A \tau_0 W_{1,-1/2} = 1 \times 10^7$ are the same for both curves.

ure 5 displays the polarization degree of PL in the Faraday and Voigt geometries. In the Faraday geometry, the PL signal is strongly circular polarized in the magnetic field higher than 2.5 T, whereas that in the Voigt geometry is almost not polarized: The spectra show a weak linear polarization degree $P_l = (I_{\perp} - I_{\parallel}) / (I_{\perp} + I_{\parallel})$ that does not exceed 0.2 as it is clear from Fig. 5. Here I_{\parallel} and I_{\perp} are the intensities of light polarized parallel and perpendicular to the direction of magnetic field. The small polarization degree P_l is the consequence of the substantial heavy-light holes splitting in disk-shaped QDs due to the strain effect, strong size quantization and heavy holes spin alignment normal to the QDs plane. A marked polarization appears only at high fields enough to markedly mix heavy and light hole states. The latter occurs when the splitting induced by the magnetic field is comparable with or larger than the splitting of heavy and light hole states.¹¹

As was discussed in introduction, two models were suggested for an explanation of magnetic field dependence of exciton emission intensity. These are (i) the suppression of Auger recombination of excitons in high magnetic field due to relaxation of Mn ions into the ground state with

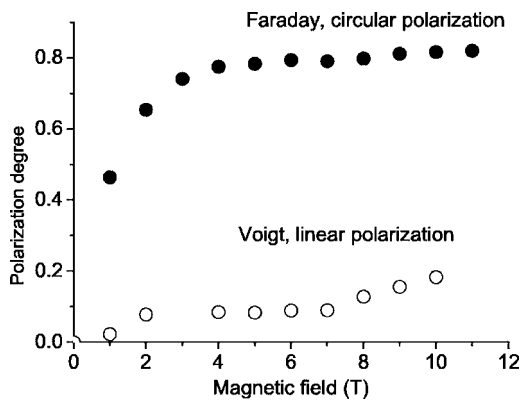


FIG. 5. Polarization degree of the PL signal vs magnetic field in the Faraday and Voigt geometries. The excitation power $P \approx 2$ mW.

$S_z = -5/2$ from which transitions into excited states T_1 with $S_z = 3/2$ demanding change of S_z are forbidden⁵ and (ii) the dissociation of D^0X centers whose Auger recombination is allowed. The dissociation occurs at magnetic fields when the energy ΔE_e of a D^0X electron in the excited spin state $\sigma_z = 1/2$ approaches its binding energy E_{BE} .⁶ The first model does not explain the magneto-optical anisotropy of the energy transfer from excitons to Mn ions observed when the magnetic field is switched from the Faraday to Voigt geometry. To test the validity of the second model for description of our experimental results we analyzed the dependence $I(B)$. The D^0X dissociation is to be proportional to $\exp((E_{BE} - \Delta E_e(B))/k_B T)$, k_B is the Boltzmann constant, and T is the temperature. Due to a very low temperature $T = 1.8$ K the effective dissociation of D^0X centers is expected in narrow range of magnetic fields providing as small change in ΔE_e as $2 - 3k_B T_{\text{eff}} \leq 2$ meV, where $T_{\text{eff}} = T + T_0$, appears due to the use of modified Brillouin function.¹⁰ It is seen in Fig. 2 that the strong variation of emission intensity is observed in the whole range of B where the change of ΔE_e exceeds 6 meV. A random distribution of the donors among QDs also decreases the probability of the Auger process with D^0X centers.⁶ Thus, we have to exclude the explanation of the magnetic field dependence of exciton emission by the model of bound excitons.

IV. SELECTION RULES FOR AN ENERGY TRANSFER FROM A QD ELECTRON-HOLE PAIR TO MN IONS

An effect of an external magnetic field on a QD electron and Mn ion spins does not depend on the magnetic field direction. Thereby it is natural to suggest that the difference in the QD emission intensity at various directions of the magnetic field is related with the hole spin behavior.

The mechanism of spin-dependent electron-hole recombination through Mn^{2+} states was proposed for the first time in the paper of Abramihvili *et al.*⁴ According to it, the nonradiative recombination of excitons in DMS structures can be accompanied with simultaneous excitation of Mn ions.

This idea was applied by Nawrocki *et al.*⁵ for the explanation of the experimental results on magnetophotocconductivity in a bulk CdMnS crystal. They considered the transition of a single photogenerated conduction electron to the valence band with simultaneous excitation of the Mn ion from the ground state 6A_1 (total spin $S=5/2$) to the first excited state 4T_1 ($S=3/2$) located about 2 eV above via the direct Coulomb interaction. The selection rules were deduced neglecting the orbital moment of electrons in valence band and Mn ones. According to the model the total spin of Mn ion+electron and its projection conserve during the Auger recombination, while the angular moment of Mn and hole states are out of consideration. Besides this, the exciton effect was also omitted and Auger transitions with electron spin-flip were not considered.

The selection rules obtained by Nawrocki *et al.* were used for the explanation of the strong increase of the exciton PL intensity with B in DMS QDs.² A good agreement with experimental data was found serious simplifications inside the

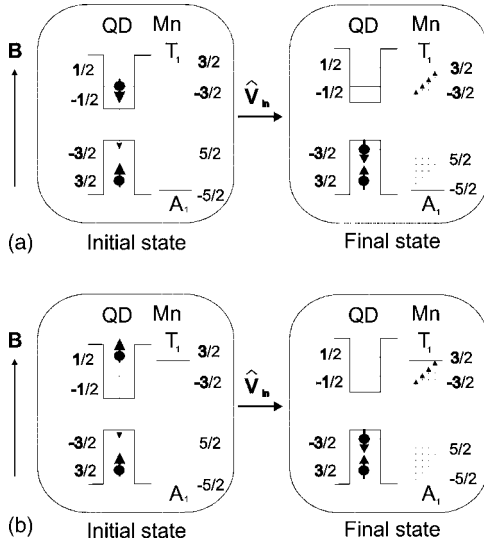


FIG. 6. Schematic picture of the Auger transitions between initial and final states of the combined system with the lowest in the magnetic field $\mathbf{B} \parallel \mathbf{0z}$ (a) “bright” and (b) “dark” exciton states. V_{in} is the interaction operator [see. Eq. (2)]. Allowed Auger transitions are shown by arrows.

model⁵ indicated above. Electron and hole spin states in DMS QDs become completely polarized in the relatively low magnetic field ~ 1 to 2 T due to the giant Zeeman splitting. Further increase of the magnetic field polarizes Mn ion states as well. At the condition of thermoequilibrium, the initially equal population of the Mn states changes exponentially with the magnetic field $\propto \exp(-g_{\text{Mn}}\mu B(S_z + 5/2)/k_B T)$. The suppression of Auger recombination in the magnetic field and strong increase of the PL intensity is explained by the exponential depopulation of Mn ion lowest state 6A_1 with $|S_z| \leq 3/2$.

This model, however, fails to explain the weak change of $I(B)$ in the Voigt geometry. Indeed, in a high magnetic field both Mn ion and electron spins are fully polarized and directed along the magnetic field. Hence, there should be no difference between the Faraday and Voigt geometries.

To explain the appearing difference one has to take into account the orbital moment of d -shell and valence band electrons as well as the spin-orbit interaction. The ground multi-electron state of the Mn^{2+} d -shell in the tetrahedral crystal field T_d is 6A_1 with the total spin $S=5/2$ and the total moment $L=0$. The nearest excited state 4T_1 ($S=3/2$) is a triplet originating from 9×4 times degenerate ${}^4G(L=4)$ atomic level split into 4 multiplets in the crystal field. The next excited state is the triplet 4T_2 located ~ 2 eV above. The spin-orbit interaction splits 4T_1 , 4T_2 , and 6A_1 states into appropriate sets of Γ_6 , Γ_7 , and Γ_8 states. However, the spin-orbit splitting is very small ($< 200 \mu\text{eV}$) and can be omitted.

We are interested in the transitions between the states of the combined system of the Mn^{2+} ion+exciton localized in a disk-shaped single QD of D_{2d} or lower symmetry caused by the Coulomb interaction between them. This process is schematically shown in Fig. 6. Although this transition is phonon-assisted the selection rules are determined mainly by the resonant process. We consider an ideal single QD with

nondegenerate valence band and the characteristic lateral dimension d comparable with the exciton Bohr radius.

The wave functions of d -electrons located on a Mn ion in CdSe have T_d symmetry. As the diameter of Mn ion $a_{\text{Mn}} \approx 1.8 \text{ \AA}$ is substantially smaller than characteristic QD size, one can neglect the splitting of the 4T_1 triplet due to the symmetry reduction. We want to stress ones attention on the fact that the orbital moment and spin are not “good” quantum numbers in the combined system due to the strong spin-orbit interaction in the valence band and quenching of the atomic orbital moment in the crystal field.

The Hamiltonian of the combined system at zero magnetic field is

$$\hat{H} = \hat{H}_{\text{Mn}} + \hat{H}_c + \hat{V}_{\text{in}}, \quad (1)$$

where $\hat{H}_{\text{Mn}} = \hat{H}_0 + \sum_i^5 U(\mathbf{R}_i)$ is the Hamiltonian of the d -shell in the strong T_d crystal field, \hat{H}_0 is the Hamiltonian of the d -shell of a free Mn ion, $U(\mathbf{R}_i)$ is the periodic part of the crystal potential; \hat{H}_c is the Hamiltonian of the QD multi-electron system which eigenstates are the Hartree-Fock states constructed from the solutions of effective mass equations for electrons in the QD. The last term in the Hamiltonian $\hat{V}_{\text{in}} = \sum_j \sum_i^5 e^2 / \epsilon_0 |\mathbf{R}_i - \mathbf{r}_j|$ describes interaction between d -shell and QD's electrons which can be treated as a perturbation for both parts of the combined system. The coordinates of the QDs and Mn electrons are \mathbf{r}_j and \mathbf{R}_i , respectively, ϵ_0 is the static dielectric constant of the media.

We will work within the framework of the strong crystal field approximation^{12–14} undermining that the crystal field $\sum_i^5 U(\mathbf{R}_i)$ is stronger than the mutual interaction of $3d^5$ electrons given by \hat{H}_0 . Then, the d shell wave functions are eigenstates of \hat{H}_{Mn} , whereas exciton ones are eigenstates of \hat{H}_c .

In a relatively strong magnetic field in the Faraday geometry the initial and final states are nondegenerate and characterized, respectively, by Mn-ion spin and exciton moment projections S_z and J_z on $\mathbf{0z}$. The appropriate wave functions are merely products of the exciton and d -shell states.

The matrix element of the Auger transition between the Mn-ion+exciton initial state (S_z, J_z) and excited final state (S'_z) is:

$$M_{0i}(J_z, S_z; S'_z) = \langle T_{1i}(S'_z) \Psi_0 | \hat{V}_{\text{in}} | A_1(S_z) \Psi_{\text{ex}}^{J_z} \rangle \quad (2)$$

In the ground state of QD, Ψ_0 , the valence band is filled while the conduction band is empty. The lowest excited state of the QD, heavy hole exciton, is an e - h pair localized within the QD where the electron and the heavy hole occupy the lowest quantization levels.¹⁵ The wave function of exciton is $\Psi_{\text{ex}}^{J_z} = c_{c\sigma_z}^+ c_{v j_z} |0\rangle$, where $c_{c\sigma_z}^+$, $c_{v j_z}$ are creation and annihilation operators of a QD conduction or valence band electrons, respectively, σ_z, j_z are projections of spin and orbital moment of conduction or valence electrons, $J_z = \sigma_z + j_z$ is the exciton moment projection. In the vacuum state $|0\rangle$ the valence band is completely filled, while the conduction band and d -shell states of the Mn ion are empty.

The spatial parts of electron wave functions in the conduction and valence bands of the disk-shaped QD are of the form:

$$\varphi_{v,c}(\mathbf{r}) = \frac{1}{\sqrt{V}} w_{c,v}(\mathbf{r}) g_{c,v}(\mathbf{r}_\perp, z) \quad (3)$$

where $\mathbf{r}_\perp = x\mathbf{e}_x + y\mathbf{e}_y$ is the in-plane part of \mathbf{r} , $w_{c,v}(\mathbf{r})$ are periodic parts of appropriate Bloch functions, $g_{c,v}(\mathbf{r}_\perp, z)$ are envelope functions and V is the integration volume.

In the strong crystal field approximation S and S_z remain to be characteristics of Mn ion states whereas L and L_z do not any more. These quantum numbers have to be replaced by filling numbers of appropriate one-electron states $|\xi\rangle, |\eta\rangle, |\zeta\rangle, |u\rangle, |v\rangle$ which one-electron wave functions belonging to T_2 and E representations of T_d symmetry group¹²⁻¹⁴ are presented in Appendix A.

Particularly, the wave function of the $A_1(-5/2)$ state of Mn ion in the strong crystal field approximation is $-a_{\xi\downarrow}^+ a_{\eta\downarrow}^+ a_{\zeta\downarrow}^+ a_{u\downarrow}^+ a_{v\downarrow}^+ |0\rangle$, where $a_{\xi\downarrow}^+, a_{\eta\downarrow}^+, a_{\zeta\downarrow}^+, a_{u\downarrow}^+, a_{v\downarrow}^+$ are creation operators of appropriate one-electron states.^{13,14} Arrows \uparrow and \downarrow denote the spin states with projections $1/2$ and $-1/2$, respectively. The other states $A_1(S_z)$ with $S_z > -5/2$, can be found by applying the spin step-up operator $\hat{S}_+ = \hat{S}_x + i\hat{S}_y$ to the $A_1(-5/2)$ wave function. For instance,

$$\begin{aligned} A_1(-3/2) &= \hat{S}_+ A_1(-5/2) \\ &= -1/\sqrt{5} (a_{\xi\uparrow}^+ a_{\eta\downarrow}^+ a_{\zeta\downarrow}^+ a_{u\downarrow}^+ a_{v\downarrow}^+ + a_{\xi\downarrow}^+ a_{\eta\uparrow}^+ a_{\zeta\downarrow}^+ a_{u\downarrow}^+ a_{v\downarrow}^+ \\ &\quad + a_{\xi\downarrow}^+ a_{\eta\downarrow}^+ a_{\zeta\uparrow}^+ a_{u\downarrow}^+ a_{v\downarrow}^+ + a_{\xi\downarrow}^+ a_{\eta\downarrow}^+ a_{\zeta\downarrow}^+ a_{u\uparrow}^+ a_{v\downarrow}^+ \\ &\quad + a_{\xi\downarrow}^+ a_{\eta\downarrow}^+ a_{\zeta\downarrow}^+ a_{u\downarrow}^+ a_{v\uparrow}^+) |0\rangle. \end{aligned}$$

The interaction \hat{V}_{in} splits the final state $|T_1(S'_z)\Psi_0\rangle$ into the states of a lower, D_{2d} , symmetry. The splitting is very small and will be omitted.

Since any combinations of d -electron wave functions are even the odd part originates from the admixture of a fraction of $4p$ state $\Phi(3d^5) = \Phi_0(3d^5) + \beta\chi(3d^4 4p)$, where $\beta \ll 1$.^{12,14} The wave functions of the T_1 triplet in the explicit form are given in Appendix A.

The states of the combined system $|A_1(S_z)\Psi_{ex}^J\rangle = C_{A_1(S_z)}^+ c_{\sigma_z}^+ c_{v_j z} |0\rangle$, $|T_{1i}(S'_z)\Psi_0\rangle = C_{T_{1i}(S'_z)}^+ |0\rangle$. Here $C_{A_1(S_z)}^+, C_{T_{1i}(S'_z)}^+$ are creation operators of $A_1(S_z), T_{1i}(S'_z)$ states (see Appendix A).

The part of interaction operator responsible for the Auger recombination of excitons is $\hat{V}'_{in} = \sum_{\sigma_z, \sigma'_z} \sum_{j_z} \sum_{\mu \neq \nu} (V_{\mu c v \nu} a_{\mu \sigma_z}^+ c_{\sigma'_z}^+ a_{\nu \sigma'_z} c_{v_j z} + V_{\mu c v \nu} a_{\mu \sigma_z}^+ c_{\sigma'_z}^+ c_{v_j z} a_{\nu \sigma'_z})$, where $a_{\nu \sigma'_z}^+, a_{\mu \sigma_z}$ are creation and annihilation operators of the d -shell electrons. The pairs of operators $c_{\sigma_z, v_j z}^+, c_{\sigma_z, v_j z}$ and $a_{\mu \sigma_z}, a_{\mu \sigma'_z}^+$ possess ordinary commutational relations. Matrix elements $V_{\mu c v \nu} = \int \psi_\mu^*(r_1) \varphi_c^*(r_2) V(\mathbf{r}_1 - \mathbf{r}_2) \psi_\nu(r_1) \varphi_v(r_2) d\mathbf{r}_1 d\mathbf{r}_2$, where $V(\mathbf{r}_1 - \mathbf{r}_2) = e^2 / \epsilon_0 |\mathbf{r}_1 - \mathbf{r}_2|$, $\psi_\mu(r)$ and $\varphi_v(r)$ are one-electron wave functions of d -shell and QD electrons, respectively.

The wave functions of electrons are not orthogonal to those of the d -electrons, which means that the anticommutator $[a_{\mu}^+ c_{c,v}]_+ = \langle \phi_\mu | \psi_{c,v} \rangle$ ¹⁶ The overlap integrals are small $\langle \phi_\mu | \psi_{c,v} \rangle \sim (a_{Mn}^3 / V_{ex})^{1/2} \ll 1$, where V_{ex} is the volume of the exciton. Hence, the contribution of nonorthogonality into the matrix element given by Eq. (2) is negligible.

Using the above wave functions one can find matrix elements of transitions $|A_1(S_z)\Psi_{ex}^1\rangle \rightarrow |T_{1i}(S'_z)\Psi_0\rangle$. The lowest state of the system in the magnetic field is $|A_1(-5/2)\Psi_{ex}^1\rangle$, the next one is $|A_1(-3/2)\Psi_{ex}^1\rangle$. Let us first calculate the matrix element of the process $|A_1(-3/2)\Psi_{ex}^1\rangle \rightarrow |T_{1i}(-3/2)\Psi_0\rangle$, where $i=x, y, z$ denotes T_1 triplet states which transforms as x, y, z , respectively, under operations of the T_d group.

The matrix elements $M_{0i}(1, -5/2, -3/2)$ of the transition from the lowest state into $T_{1x,y}(-3/2)$ ones are determined by the expression

$$\begin{aligned} & \mp \frac{1}{2} \langle \theta(\mathbf{r}_1) \uparrow \varphi_v(\mathbf{r}_2) \downarrow | V(\mathbf{r}_1 - \mathbf{r}_2) | v(\mathbf{r}_1) \uparrow \varphi_c(\mathbf{r}_2) \downarrow \rangle \\ & + \frac{\sqrt{3}}{2} \langle \theta(\mathbf{r}_1) \uparrow \varphi_v(\mathbf{r}_2) \downarrow | V(\mathbf{r}_1 - \mathbf{r}_2) | u(\mathbf{r}_1) \uparrow \varphi_c(\mathbf{r}_2) \downarrow \rangle, \quad (4) \end{aligned}$$

where $\theta = \xi, \eta$ for $i=x, y$, respectively. The upper sign corresponds to $i=x$, whereas the lower to $i=y$.

The matrix element for the transition into ${}^4T_{1z}(-3/2)$ state is

$$\frac{1}{2} \langle \zeta(\mathbf{r}_1) \uparrow \varphi_v(\mathbf{r}_2) \downarrow | V(\mathbf{r}_1 - \mathbf{r}_2) | v(\mathbf{r}_1) \uparrow \varphi_c(\mathbf{r}_2) \downarrow \rangle, \quad (5)$$

These matrix elements show that it is the direct interaction which is responsible for the allowed Auger transitions involving bright excitons whereas the exchange interaction results in the allowed transitions with participation of dark excitons.

The matrix elements given by Eqs. (4) and (5) can be interpreted as a recombination of an e - h pair with simultaneous excitation of one d -electron from e to t_2 level via the direct Coulomb interaction.¹⁷

The matrix elements allows us to determine the selection rules for the Auger process. Thus, for the bright exciton the transitions are allowed when $S'_z = S_z$ which coincides with those found in Ref. 5. Consequently, transitions involving the bright exciton and the lowest Mn Zeeman level ($|A_1(-5/2)\Psi_{ex}^1\rangle \rightarrow |T_{1i}(S'_z)\Psi_0\rangle$) are forbidden, while transitions from the next level ($|A_1(-3/2)\Psi_{ex}^1\rangle \rightarrow |T_{1i}(-3/2)\Psi_0\rangle$) are allowed. In general, for the dark exciton with $J_z = \pm 2$ Auger transitions are allowed when $S'_z = S_z \pm 1$, respectively. It means that unlike the bright exciton the transition for $A_1(-5/2) +$ dark exciton is allowed.

Thus, the increase of the PL intensity with the magnetic field in the Faraday geometry is the result of the fast relaxation of dark excitons into the lowest bright exciton state and depopulation of the upper exciton states. The inclined magnetic field mixes bright and dark exciton states. It is the admixture of $J=2$ state to the ground $J=1$ state which is the main reason of the short Auger recombination time observed in the Voigt geometry.

The dependance of matrix elements of Auger transitions spin polarized exciton and Mn ion states in the Faraday ge-

ometry allows one to find matrix elements in the Voigt geometry since the exciton states in this case are superposition of various J, J_z states.

The selection rules obtained for QDs are also valid for QWs as it is shown in Appendix B.

V. COMPARISON WITH THE EXPERIMENT

Magnetic field $\mathbf{B} \parallel \mathbf{0z}$ quickly depopulates excited QD's exciton spin states.

In the case of relatively slow Auger process, the lifetime of the lowest $J_z=1$ state can be written as

$$\frac{1}{\tau} = \frac{1}{\tau_A} + \frac{1}{\tau_0}, \quad (6)$$

where τ_0 and τ_A are the times of radiative and nonradiative recombinations of the exciton, respectively.

The exciton PL intensity in the Faraday geometry is described as²

$$\frac{I(B)}{I(0)} = \frac{\text{const}}{1 + (\tau_0/\tau_A)} \quad (7)$$

The effective time of nonradiative recombination depends on B as

$$1/\tau_A = N_A \sum_{J_z, S_z} W_{J_z, S_z} p_{\text{ex}}^{J_z}(B) p_{\text{Mn}}^{S_z}(B) \quad (8)$$

where the probabilities of Auger transition from the ground ($J_z=1, S_z=-5/2$) into the final ($S_z=\pm 3/2, \pm 1/2$) state $W_{J_z, S_z} \propto |\sum_i M_{0i}(J_z, -5/2, S_z)|^2$ since the splitting of T_{1i} states in the magnetic field is negligibly small. Here $p_{\text{ex}}^{J_z}(B), p_{\text{Mn}}^{S_z}(B)$ are occupation probabilities of the appropriate exciton states and Mn ground state, $N_A = xN_0V_{\text{eff}}$ is the number of Mn ions within the effective volume V_{eff} . The probability of an arbitrary Mn ion to occupy the energy levels $A_1(S_z)$ is

$$p_{\text{Mn}}^{S_z} = \frac{1}{Q_{\text{Mn}}} e^{-\lambda S_z}, \quad (9)$$

where

$$Q_{\text{Mn}} = \frac{\sinh(3\lambda)}{\sinh(\lambda/2)}, \quad \lambda = \frac{g_{\text{Mn}}\mu_B B}{kT}.$$

The probability $p_{\text{ex}}^{J_z}$ can be expressed as:

$$p_{\text{ex}}^{J_z}(B) = \frac{1}{Q_{\text{ex}}} \exp\left(\frac{-\Delta E_Z(J_z)}{kT}\right) \quad (10)$$

$$Q_{\text{ex}} = \sum_{J_z} p_{\text{ex}}^{J_z}$$

where $\Delta E_Z(J_z) = |E_Z(J_z) - E_0|$ is the absolute value of the exciton line shift, E_0 is the line position at $B=0$. The value of $\Delta E_Z(J_z)$ can be found from the transient shift of the exciton line in PL spectra presented in Fig. 3.

So far we have considered a single Mn ion interacting with a single QD. In reality, every exciton interacts with $N = x_{\text{eff}}N_0V_{\text{eff}}$ Mn ions, localized within some effective volume

V_{eff} compatible with the volume of the exciton and the Auger transition rate depends on N . Here N_0 is the number of cations per unit cell, x_{eff} is the effective Mn mole content. In the latter case the PL shift is well described by the expression:^{8,9}

$$E_Z(J_z) - E_0 = -\mathbf{B}_{\text{ex}} \mathbf{M}(B, T_{\text{eff}}) V_{\text{eff}}, \quad (11)$$

where $\mathbf{B}_{\text{ex}} = \mathbf{B}_{\text{ex}}^h + \mathbf{B}_{\text{ex}}^e$ is the effective exchange field describing the exchange interaction with Mn ions localized within V_{eff} , $\mathbf{B}_{\text{ex}}^e = \alpha \sigma_z / (2V_{\text{eff}})$, $\mathbf{B}_{\text{ex}}^h = -\beta \mathbf{j}_z / (3V_{\text{eff}})$ are electron and hole exchange fields, α, β are electron and hole exchange parameters, respectively; $\mathbf{M}(B, T_{\text{eff}}) = -5/2 x_{\text{eff}} N_0 B r_{5/2} (5g_{\text{Mn}} \mu_B B / 2kT_{\text{eff}}) \mathbf{B} / B$ is the magnetization. $T_{\text{eff}} = T + T_0$, the temperature T_0 appears due to the antiferromagnetic interaction between Mn ions.¹⁰ The exchange interaction between the exciton and Mn ions at helium temperatures leads to the formation of exciton magnetic polaron.^{8,9} The formula (11) is valid in this case if one changes \mathbf{B} to $\mathbf{B}_{\Sigma} = \mathbf{B} + \mathbf{B}_{\text{ex}}$. In the inhomogeneous ensemble, CdMnSe QDs differ in their dimensions, local Mn content and strain distribution. These factors lead to a broad line usually observed in PL spectra (see Fig. 2). Due to the strong anisotropy of the disk-shaped QDs and relatively large lateral sizes we can describe them as a quantum wells with broken translational symmetry. Thus, the hole Hamiltonian of the semimagnetic quantum disk is equal to

$$\begin{pmatrix} E_{hh} + 3G & 0 & 0 & 0 \\ 0 & E_{lh} + G & 0 & 0 \\ 0 & 0 & E_{lh} - G & 0 \\ 0 & 0 & 0 & E_{hh} - 3G \end{pmatrix} \quad (12)$$

in the $|j, j_z\rangle$ basis.^{6,11} Here $G = 1/3 B_{\text{ex}}^h M(B, T_{\text{eff}})$.

In QDs with a lateral dimensions d of 10–20 nm the k uncertainty $\Delta k \leq 1/d \sim 10^6 \text{ cm}^{-1}$ and the influence of the lateral dimensional quantization is negligible.

In the Faraday geometry the magnetic field does not mix the basis states and the Zeeman splitting does not depend on E_{hh} and E_{lh} . Thus, $I(B)$ of the QDs ensemble is described well by the expression (7).

The fit of the spectral shift of the maximum of PL signal with formula (11) is presented Fig. 3. Four free parameters $T_{\text{eff}}, E_0, B_{\text{ex}}, E_{mp} = -B_{\text{ex}} M(B_{\text{ex}}, T_{\text{eff}}) V_{\text{eff}}$ were used to find the best fit.^{8,9} The parameter E_{mp} has the meaning of exciton magnetic polaron binding energy at zero field.⁸

Due to a rather quick spin relaxation of excitons in DMS structures the most excitons relax into the lowest state at the magnetic field $B < 1 \text{ T}$.⁸ Thus, we can set $p_{\text{ex}}^1(B) = 1$ and zero for the others. If we leave only two terms in the Eq. (10) corresponding to the transitions from $S_z = -3/2$ and $-1/2$ levels of A_1 then $1/\tau_A \approx N_A W_{1,-3/2} p_{\text{Mn}}^{-3/2} + N_A W_{1,-1/2} p_{\text{Mn}}^{-1/2}$.

Figure 4 demonstrates good fit of the experimentally observed increase of PL in the Faraday geometry and the calculated ones obtained from Eq. (7). Three adjustable parameters $T, N_A \tau_0 W_{1,-3/2}$ and $N_A \tau_0 W_{1,-1/2}$ are used to fit the experimental data. The last two parameters are chosen to be the same for both curves.

In the Voigt geometry the hole Hamiltonian in the magnetic field $B \parallel \mathbf{0x}$ is block-diagonalized in the basis

$$(1/\sqrt{2}(|3/2, 3/2\rangle - |3/2, -3/2\rangle), 1/\sqrt{2}(|3/2, 1/2\rangle - |3/2, -1/2\rangle), 1/\sqrt{2}(|3/2, 3/2\rangle + |3/2, -3/2\rangle), 1/\sqrt{2}(|3/2, 1/2\rangle + |3/2, -1/2\rangle)$$

$$\begin{pmatrix} E_{hh} & \sqrt{3}G & 0 & 0 \\ \sqrt{3}G & E_{lh} - G & 0 & 0 \\ 0 & 0 & E_{lh} + G & \sqrt{3}G \\ 0 & 0 & \sqrt{3}G & E_{hh} \end{pmatrix}$$

The wave function of the lowest energy state is $\varphi_0 = \chi_{hh}/\sqrt{2}(|3/2, 3/2\rangle - |3/2, -3/2\rangle) + \chi_{lh}/\sqrt{2}(|3/2, 1/2\rangle - |3/2, -1/2\rangle)$, where coefficients $\chi_{hh} = -\sqrt{3}G/\sqrt{(E_{hh}-E)^2+3G^2}$, $\chi_{lh} = (E_{hh}-E)/\sqrt{(E_{hh}-E)^2+3G^2}$, $E = 1/2(E_{hh}+E_{lh}+2G) + \sqrt{1/4(E_{hh}-E_{lh}-2G)^2+3G^2}$.

As was mentioned above, polarization measurements in the Voigt geometry showed that the linear polarization of QD emission does not exceed 20% at 11 T. That means that the magnetic field of 11 T is not enough to change the direction of the hole spin in the investigated QDs because the splitting of light and heavy holes in highly strained and thin QDs is markedly higher than the splitting induced by the magnetic field. The main effect of the magnetic field parallel to the QD plane is the mixing of bright and dark exciton states. Indeed, the lowest conduction electron states in the magnetic field is a combination of $|\pm 1/2\rangle$ states and, hence, the lowest exciton state consist of a mixture of bright and dark excitons with $J_z = \pm 1, 2$. The admixture of dark $J=2$ component to the ground exciton state provides an enhanced Auger recombination in the Voigt geometry.

Thus, the increase of $I(B)$ in the Faraday geometry is determined by the splitting of Mn spin states, whereas in the Voigt geometry it is connected mainly with the decrease of part of the $J=2$ component with B . The strong dependence of the light-heavy hole splitting on QD thickness results in a strong dispersion of Auger recombination rate of QD ensemble in the Voigt geometry and does not allow any quantitative fit. The latter will be possible in the case of a single QD emission investigations.

VI. CONCLUSIONS

PL from the sample containing MBE grown CdMnSe-ZnSe QDs was measured in the magnetic field up to 11 T perpendicular and parallel to the growth plane at liquid He temperatures.

The strong, about two orders of magnitude, increase of the QD PL intensity in the Faraday geometry and a much weaker, less than two times, in the Voigt one was observed. The magnetic field anisotropy in the quantum yield required a revision of suggested earlier selection rules⁵ for Auger recombination of QD excitons with excitation of Mn-ions from the ground to excited states allowing the only transitions without change of Mn ion spin projection S_z [5]. The revised selection rules were obtained taking into account the spin structure of both exciton and Mn states. It was found that in the Faraday geometry, the exciton Auger recombination with

change of S_z is forbidden only for bright excitons. In contrast, the Auger recombination of dark excitons is forbidden for transitions with $\Delta S_z=0$ and allowed for those with $\Delta S_z = \pm 1$. The suppression of Auger recombination in high magnetic fields occurs due to the fast spin relaxation of excitons into the ground bright state. In the Voigt geometry, the magnetic field mixes bright and dark exciton states. It is this mixture that provides the observed fast Auger recombination in magnetic fields parallel to the QD plane. The suggested model fits well to the experimental data in the Faraday geometry and explains the observed dependence of quantum yield of the QD exciton emission on magnetic field direction.

ACKNOWLEDGMENTS

This work was supported by the Russian Foundation for Basic Research Grant No. 04-02-17338 and INTAS. Authors are grateful to L.V. Keldish and S.N. Molotkov for the reading of the manuscript and valuable remarks. V.D.K. thanks A.A. Maksimov and D.R. Yakovlev for fruitful discussions. A.V.C. wishes to acknowledge Tatiana Balashova for inspiration during the experiments.

APPENDIX A: WAVE-FUNCTIONS OF MN ION STATE T_1

Using the methods developed in Refs. 12 and 13 and results of paper 14 $T_1(-3/2)(t_2^4e)$ wave-functions can be expressed as follows:

$$|T_{1x}(-3/2)\rangle = \left(-\frac{1}{2}a_{\xi\downarrow}^+a_{\xi\uparrow}^+a_{\eta\downarrow}^+a_{\eta\uparrow}^+a_{u\downarrow}^+ + \frac{\sqrt{3}}{2}a_{\xi\downarrow}^+a_{\xi\uparrow}^+a_{\eta\downarrow}^+a_{\eta\uparrow}^+a_{v\downarrow}^+ \right) |0\rangle \quad (\text{A1})$$

$$|T_{1y}(-3/2)\rangle = \left(\frac{1}{2}a_{\xi\downarrow}^+a_{\eta\uparrow}^+a_{\eta\downarrow}^+a_{\xi\uparrow}^+a_{u\downarrow}^+ + \frac{\sqrt{3}}{2}a_{\xi\downarrow}^+a_{\eta\uparrow}^+a_{\eta\downarrow}^+a_{\xi\uparrow}^+a_{v\downarrow}^+ \right) |0\rangle \quad (\text{A2})$$

$$|T_{1z}(-3/2)\rangle = (a_{\xi\downarrow}^+a_{\eta\downarrow}^+a_{\xi\uparrow}^+a_{\eta\uparrow}^+a_{u\downarrow}^+) |0\rangle \quad (\text{A3})$$

where

$$a_u^+|0\rangle = \langle r|d_{z^2}\rangle = R_{3d}(r) \left(\frac{5}{4\pi} \right)^{1/2} \left(\frac{3z^2 - r^2}{2r^2} \right),$$

$$a_v^+|0\rangle = \langle r|d_{x^2-y^2}\rangle = R_{3d}(r) \left(\frac{15}{4\pi} \right)^{1/2} \left(\frac{x^2 - y^2}{2r^2} \right)$$

belongs to e representation of T_d point group, whereas

$$a_{\xi}^+|0\rangle = \langle r|d_{yz}\rangle - \gamma\langle r|p_x\rangle,$$

$$a_{\eta}^+|0\rangle = \langle r|d_{zx}\rangle - \gamma\langle r|p_y\rangle,$$

$$a_{\zeta}^+|0\rangle = \langle r|d_{xy}\rangle - \gamma\langle r|p_z\rangle,$$

belong to t_2 representation. Here $\langle r|d_{yz}\rangle = R_{3d}(r) \times (15/4\pi)^{1/2}(yz/r^2)$, $\langle r|d_{zx}\rangle = R_{3d}(r)(15/4\pi)^{1/2}(zx/r^2)$, $\langle r|d_{xy}\rangle = R_{3d}(r)(15/4\pi)^{1/2}(xy/r^2)$, $\langle r|p_x\rangle =$

$-iR_{4p}(3/4\pi)^{1/2}(x/r)$, $\langle r|p_y\rangle = -iR_{4p}(r)(3/4\pi)^{1/2}(y/r)$, $\langle r|p_z\rangle = -iR_{4p}(3/4\pi)^{1/2}(z/r)$; $R_{3d}(r)$ and $R_{4p}(r)$ are the spatial parts of atomic $3d$ and $4p$ -electron wave-functions. The coefficient $\gamma = \langle 3d_{xy}|V_{\text{odd}}|4p_z\rangle / (E_{4p}^0 - E_{3d}^0) \sim 1/10$, where E_{3d}^0 , E_{4p}^0 are the energies of p and d -orbitals, $V_{\text{odd}} \propto xyz$ is the odd parity part of the crystal field potential.^{12,13}

The Mn d -shell states can be presented in the form $|T_{1i}\rangle = C_{T_{1i}}^+|0\rangle$, $|A_1\rangle = C_{A_1}^+|0\rangle$, where $C_{T_{1i}}^+$, $C_{A_1}^+$ have the meaning of creation operators of d^5 shell states and are given by the expressions in the brackets in Eqs. (A1)–(A3).

APPENDIX B: MATRIX ELEMENTS OF THE AUGER TRANSITION IN QW

The wave function of a QW exciton with J_z is

$$\Psi_{\text{ex}}^{J_z}(\mathbf{K}) = \sum_{\mathbf{k}_c, \mathbf{k}_v} A(\mathbf{k}_c, \mathbf{k}_v) c_{\mathbf{k}_c, \sigma_z}^+ c_{v, \mathbf{k}_v, j_z} |0\rangle,$$

where $\mathbf{k}_{c,v}$ are the in-plane quasi-moments of electrons in conduction and valence bands, $\mathbf{K} = \mathbf{k}_c - \mathbf{k}_v$.

$$\sum_{\mathbf{k}_c, \mathbf{k}_v} A(\mathbf{k}_c, \mathbf{k}_v) e^{i(\mathbf{k}_c \mathbf{r}_1 + \mathbf{k}_v \mathbf{r}_2)} = F(\mathbf{r}_1 - \mathbf{r}_2),$$

where $F(\mathbf{r}_1 - \mathbf{r}_2)$ is the exciton envelope function.

In a narrow QW the valence band is not degenerate and the dispersion low is parabolic at small \mathbf{k}_v . The wave functions of conduction and valence electrons are as follows:

$$\varphi_{c, \mathbf{k}_c, \sigma_z, v, \mathbf{k}_v, j_z}(\mathbf{r}) = c_{c, \mathbf{k}_c, \sigma_z}^+ c_{v, \mathbf{k}_v, j_z} |0\rangle = w_{c,v}(\mathbf{r}) g_{c,v}(z) \frac{1}{\sqrt{S}} e^{i\mathbf{k}_{c,v} \cdot \mathbf{r}_\perp},$$

where the in-plane vector $\mathbf{r}_\perp = x\mathbf{e}_x + y\mathbf{e}_y$. These wave functions are not orthogonal to the d -electron ones. The overlap integral between them, however, is small and can be omitted. The matrix element of the Auger transition involving $A_1(-3/2)$ state into the $T_{1x}(-3/2)$ state via the direct Coulomb interaction is

$$F(0) \left(-\frac{1}{2} \langle e^{-i\mathbf{K} \cdot \mathbf{r}_2} \xi(\mathbf{r}_1) \uparrow \phi_v(\mathbf{r}_2) \downarrow | V(1,2) | v(\mathbf{r}_1) \uparrow \phi_c(\mathbf{r}_2) \downarrow \rangle + \frac{\sqrt{3}}{2} \langle e^{-i\mathbf{K} \cdot \mathbf{r}_2} \xi(\mathbf{r}_1) \uparrow \phi_v(\mathbf{r}_2) \downarrow | V(1,2) | u(\mathbf{r}_1) \uparrow \phi_c(\mathbf{r}_2) \downarrow \rangle \right)$$

Considering the transitions involving the dark exciton $J_z=2$ into the $T_{1x}(-3/2)$ state we obtain:

$$- \left(-\frac{1}{2} \langle F(\mathbf{r}) e^{-i\mathbf{K} \cdot \mathbf{R}} \xi(\mathbf{r}_2) \uparrow \phi_v(\mathbf{r}_1) \downarrow | V(1,2) | v(\mathbf{r}_1) \downarrow \phi_c(\mathbf{r}_2) \uparrow \rangle + \frac{\sqrt{3}}{2} \langle F(\mathbf{r}) e^{-i\mathbf{K} \cdot \mathbf{R}} \xi(\mathbf{r}_2) \uparrow \phi_v(\mathbf{r}_1) \downarrow | V(1,2) | u(\mathbf{r}_1) \downarrow \phi_c(\mathbf{r}_2) \uparrow \rangle \right),$$

where $\mathbf{R} = (m_c \mathbf{r}_1 + m_v \mathbf{r}_2) / (m_c + m_v)$, $\mathbf{r} = \mathbf{r}_1 - \mathbf{r}_2$.

The matrix elements of the transitions into $T_{1y}(-3/2)$ and $T_{1z}(-3/2)$ states can be found in the same manner. One can find that the spin selection rules remain to be the same as in the QD case. For instance, transitions from the state $|A_1(-5/2)\rangle \Psi_{\text{ex}}^1$ are forbidden.

*Electronic address: chernen@issp.ac.ru

¹W. Heimbrodt and P. J. Klar, in *Magnetic nanostructures*, edited by H. S. Nalwa, (American Scientific Publishers, California 2002), pp. 1–58.

²C. S. Kim, M. Kim, S. Lee, J. Kossut, J. K. Furdyna, and M. Dobrowolska, *J. Cryst. Growth* **214/215**, 395 (2000).

³K. Shibata, E. Nakayama, I. Souma, and Y. Oka, *Phys. Status Solidi A* **229**, 473 (2002).

⁴V. G. Abramishvili, A. M. Komarov, S. M. Ryabchenko, and Yu. G. Semenov, *Solid State Commun.* **78**, 1069 (1991).

⁵M. Nawrocki, Yu. G. Rubo, J. P. Lascaray, and D. Coquillat, *Phys. Rev. B* **52**, R2241 (1995).

⁶H. Falk, J. Hübner, P. J. Klar, and W. Heimbrodt, *Phys. Rev. B* **68**, 165203 (2003).

⁷A. V. Chernenko, P. S. Dorozhkin, V. D. Kulakovskii, A. S. Brichkin, S. V. Ivanov, and A. A. Toropov, *11th International Symposium Nanostructures: Physics and Technology* (Ioffe Institute, 2003), pp. 360–361.

⁸P. S. Dorozhkin, A. V. Chernenko, V. D. Kulakovskii, A. S.

Brichkin, A. A. Maksimov, H. Schoemig, G. Bacher, A. Forchel, S. Lee, M. Dobrowolska, and J. K. Furdyna, *Phys. Rev. B* **68**, 195313 (2003).

⁹G. Bacher, A. A. Maksimov, H. Schömig, V. D. Kulakovskii, M. K. Welsch, A. Forchel, P. S. Dorozhkin, A. V. Chernenko, S. Lee, M. Dobrowolska, and J. K. Furdyna, *Phys. Rev. Lett.* **89**, 127201-1 (2002).

¹⁰J. K. Furdyna, *J. Appl. Phys.* **64**, R29 (1988).

¹¹B. Kuhn-Heinrich, W. Ossau, E. Bangert, A. Waag, and G. Landwehr, *Solid State Commun.* **91**, 11 (1994).

¹²C. Ballhausen, *Introduction to Ligand Field Theory* (McGraw-Hill, New York, 1962).

¹³S. Sugano, Y. Tanabe, and H. Kamimura, *Multiplets of Transition Metal Ions* (Academic, New York, 1970).

¹⁴Nguen Que Huong and J. L. Birman, *Phys. Rev. B* **69**, 085321 (2004).

¹⁵We omit a weak effect of Coulomb interaction on $e-h$ pair because it does not change its spin states.

¹⁶Yu. G. Semenov and B. D. Shanina, *Phys. Status Solidi B* **104**,

631 (1981).

¹⁷Besides the mixing of $3d_{t_2}$ and $4p$ states of an isolated Mn ion, the crystal field mixes $3d_{t_2}$ and valence band states. This mixing is responsible for the giant Zeeman effect in DMS and the pa-

rameter of the mixing can be found from the value of the hole exchange constant β . The effect of the mixing can be comparable with that of the $3d-4p$ Mn ion mixing and increases effectiveness of the Auger recombination of bright excitons.